

Solidification Effect of an Iron-based Biochar Heavy Metal Stabilizer on River and Lake Sediments

Mingxun HOU^{1,2*}, Jiayi YANG³, Yuefei ZENG¹

¹ Guangdong Construction Polytechnic, Guangzhou, 510640, China

² Guangzhou Vocational University of Science and Technology, Guangzhou 510080, China

³ Guangdong Communication Planning & Design Institute Group Co., Ltd., Guangzhou 510080, China

<http://dx.doi.org/10.5755/j02.ms.43587>

Received 12 November 2025; accepted 29 January 2026

To address heavy metal pollution in river and lake sediments amid China's urbanization, this study developed an iron-based biochar stabilizer using corn straw modified by chemical-physical methods. The modification significantly increased the biochar's surface roughness, forming a 50–200 nm iron oxide adhesion layer. While its specific surface area slightly decreased from 418 m²/g to 376 m²/g, the proportion of mesopores rose, creating more sites for heavy metal adsorption. Characterization results show that the iron-based biochar binds heavy metals through surface functional groups like -OH and C=O, demonstrating stable adsorption performance for various heavy metals (including Cr(VI), Cd(II), Pb(II), and As(III)). Compared with unmodified biochar, it improved the average solidification rates of Zn, Cu, Cr, Pb, Ni, and As by 23.5 %, 18.7 %, 27.3 %, 25.1 %, 19.8 %, and 21.2 %, respectively. Notably, the solidification of Cr(VI) was particularly effective due to the redox catalytic action of Fe³⁺/Fe²⁺. After adsorption, the material's porosity recovered to 72 %, indicating enhanced recyclability through iron-based modification. The leaching concentration of heavy metals in the treated sediment meets national standards, and the treatment cost is over 60 % lower than that of traditional technologies. Additionally, the solidified sediment can be safely reused for land improvement or building material production, offering an economical and efficient resource-oriented solution for controlling heavy metal pollution in sediments.

Keywords: iron-based biochar, heavy metals, curing agent.

1. INTRODUCTION

In recent years, rapid urbanization and population growth have led to extensive discharge of industrial and domestic wastewater into natural water bodies. This wastewater contains high levels of nitrogen, phosphorus, and heavy metals, which accumulate in river and lake sediments. When pollution reaches a critical level, these contaminants can be re-released, causing secondary pollution and posing serious risks to ecosystems and human health [1].

Sediment plays a dual role in aquatic ecosystems: it temporarily retains pollutants through adsorption and precipitation, improving water quality, while also acting as a long-term sink for contaminants. However, continuous input of untreated pollutants has exceeded the self-purification capacity of water bodies, leading to worsening sediment pollution. This prolonged contamination threatens aquatic life and, through bioaccumulation, human health. Heavy metals, such as lead, cadmium, mercury, chromium, nickel, copper, and zinc are typical pollutants with densities above 4.5 g/cm³ [2–4].

Currently, dredging technology is widely used for river and lake sediment treatment. The conventional process involves dewatering and landfill disposal, which poses issues such as high environmental risks, low resource utilization, and land constraints. Dredged sediment consists largely of clay and fine silt, with pollutants primarily

including heavy metals and refractory organic compounds. Heavy metals are especially notable for their high biotoxicity, necessitating specialized treatment for pollution control [5–7].

Solidification/stabilization has emerged as an economical and practical solution: 1) solidification uses cementitious materials like cement to form a stable structure; 2) stabilization employs chemical additives to convert pollutants into less toxic and mobile forms, effectively preventing environmental spread [8].

As an eco-friendly material, biochar can immobilize pollutants by altering the solubility, valence state, and form of heavy metals. However, its adsorption capacity and catalytic performance are limited. To address this, researchers developed metal impregnation modification: impregnating biochar with metal salt solutions followed by pyrolysis to deposit metal oxides on its surface [9–10]. This increases specific surface area and cation charge density, significantly enhancing pollutant adsorption.

With its porous structure, tunable surface area, and abundant functional groups, biochar is key in heavy metal remediation. Iron-based biochar composites exhibit high reactivity and multiple adsorption sites, showing strong performance in treating chromium, cadmium, and mercury. Current modifications include physical (pyrolysis, ball milling), chemical (acid/base/metal treatment), and biological methods. This study innovatively combines chemical and physical approaches, using blast furnace slag and fly ash to produce iron-modified biochar. It passivates heavy metals, improves soil properties, supplements

* Corresponding author: M. Hou

E-mail address: houmingxun@gkd.edu.cn

organic matter, and regulates microbial activity, enabling contaminated soil resource utilization [11, 12].

Therefore, the main objective of this work is to develop an iron-based biochar heavy metal stabilizer using corn straw modified by combined chemical-physical methods (with blast furnace slag and fly ash as modifiers), systematically investigate its structural characteristics and heavy metal adsorption mechanisms, evaluate its stabilization efficiency for typical heavy metals (Zn, Cu, Cr, Pb, Ni, As, etc.) in river and lake sediments, and ultimately provide an economical, efficient, and resource-oriented technical solution for the remediation of heavy metal-contaminated sediments.

2. Experimental Materials and Preparation Methods

2.1. Experimental materials

The raw materials used in this experiment include industrial slag, corn stover, and river sediment. The source, key components, and basic property parameters of each raw material are as follows:

- Industrial slag: accounting for 25 % of the total weight, it consists of blast furnace slag and waste residue (fly ash) from the power industry. Among them, the main chemical components of blast furnace slag are CaO, SiO₂, Al₂O₃, and MgO, with the mass fraction of FeO/Fe₂O₃ being approximately 2 %; the main chemical components of fly ash are SiO₂, Al₂O₃, and CaO, with the mass fraction of Fe₂O₃ being about 4 %. The micro-morphology of blast furnace slag is shown in Fig. 1.



Fig. 1. Blast furnace slag

- Corn stover: after dehydration treatment, its moisture content is controlled below 10 %, and it accounts for 50 % of the total weight of experimental raw materials. The appearance morphology of corn stover is shown in Fig. 2.
- River sediment: collected from the bottom of Shijing River in Guangzhou City, samples were obtained continuously for 12 months using a monthly periodic sampling method to ensure the representativeness of the samples. The appearance morphology of the sediment is shown in Fig. 3. The statistical results of the main heavy metal contents in the sediment are presented in Table 1, where the Zn content ranges from 53.45 to 299.14 mg/kg, with an average value of 176.295 mg/kg and a standard deviation of 56.32 mg/kg; the Cu content ranges from 21.32 to

113.32 mg/kg, with an average value of 67.32 mg/kg and a standard deviation of 21.31 mg/kg;



Fig. 2. Corn straw

The Cr (the original text mistakenly wrote "Gr", which refers to chromium element) content ranges from 24.31 to 189.32 mg/kg, with an average value of 106.815 mg/kg and a standard deviation of 32.12 mg/kg; the Pb content ranges from 11.32 to 123.21 mg/kg, with an average value of 67.265 mg/kg and a standard deviation of 21.89 mg/kg; the Ni content ranges from 9.95 to 56.32 mg/kg, with an average value of 33.135 mg/kg and a standard deviation of 12.46 mg/kg; the as content ranges from 2.54 to 31.33 mg/kg, with an average value of 16.935 mg/kg and a standard deviation of 5.98 mg/kg.



Fig. 3. River sediment

Table 1. Content of major heavy metals in the sediment of Shijing river in Guangzhou city

Element name	Maximum value, mg/kg	Minimum value, mg/kg	Average value, mg/kg	Standard deviation, mg/kg
Zn	299.14	53.45	176.295	56.32
Cu	113.32	21.32	67.32	21.31
Cr	189.32	24.31	106.815	32.12
Pb	123.21	11.32	67.265	21.89
Ni	56.32	9.95	33.135	12.46
As	31.33	2.54	16.935	5.98

2.2. Preparation methods

2.2.1. Raw material pretreatment

Cleaning: rinse corn stover with deionized water to remove external impurities such as dust and soil attached to its surface, preventing impurities from interfering with

the subsequent preparation process and product performance.

Drying: transfer the cleaned corn stover to an electric blast drying oven at 90 °C for drying to initially remove moisture; in the subsequent process of preparing corn stover biochar, it needs to be dried continuously in an electric blast drying oven at 105 °C for 12 hours to ensure full removal of moisture in the stover and guarantee the stability of the subsequent pyrolysis reaction.

Crushing and Sieving: crush the dried corn stover using crushing equipment, refine the particles through grinding, and then sieve the ground material with a 100-mesh standard sieve to select particles with uniform size, ensuring sufficient material contact and consistent reaction rate in the subsequent reaction process.

Impurity removal: immerse the sieved corn stover biochar in 1 mol/L dilute hydrochloric acid for 24 hours, controlling the solid-liquid ratio at 1:100 during immersion. Dilute hydrochloric acid reacts with impurities such as soluble salts and metal oxides in the biochar to achieve impurity removal; after immersion, repeatedly wash the biochar with deionized water until the pH value of the washing solution reaches neutral, avoiding adverse effects of residual hydrochloric acid on subsequent iron loading and the performance of the stabilizer.

2.2.2. Pyrolysis treatment

Place the pretreated biomass raw material in a tube furnace, introduce N₂, heat it to a specific temperature at a certain heating rate, and maintain it for a period of time. Specifically, heat it to 200 °C at a heating rate of 10 °C/min and pyrolyze for 5 hours.

2.2.3. Iron loading-chemical solution mixing method

Disperse the biochar in ultrapure water by ultrasonic treatment: ultrasonicate the corn straw biochar in ultrapure water for 30 minutes.

Grind the blast furnace slag into powder, dissolve the powder in 500 mL of deionized water, stir with a glass rod, and then place it on a magnetic stirrer for constant temperature stirring at 40 °C for 6 hours.

Add the corn straw to the above solution, stir thoroughly for 300 minutes. After stirring, take it out and place it in an ultrasonic machine for ultrasonic oscillation for 1.5 hours. Then take out the beaker, let it stand, filter it, and place it in an electric blast drying oven for drying. Place the dried corn straw biochar under an ultraviolet lamp with a radiation wavelength of 365 nm at a distance of 60 mm for irradiation for 12 hours to prepare the iron-based modified biochar.

2.3. Key characterization methods

Scanning Electron Microscopy (SEM): GeminiSEM 300 (Carl Zeiss, Oberkochen, Germany), 5 kV working voltage, 10k–200k magnification. Samples (original biochar, iron-based biochar, post-adsorption biochar) were brittle-fractured with liquid nitrogen and gold-sprayed for 60s using JFC-1600 ion sputtering apparatus (JEOL, Tokyo, Japan).

Fourier Transform Infrared (FTIR) Spectroscopy: Nicolet iS50 (Thermo Fisher Scientific, Waltham, USA),

4000–400 cm⁻¹ wavenumber range, 32 scans, 4 cm⁻¹ resolution. Freeze-dried samples (river sediment, sediment + iron-based biochar) were mixed with KBr (1:100) for tableting.

3. Evaluation of adsorption effect of iron-based biochar

3.1. Material characterization and analysis

A scanning electron microscope was used to characterize the original biochar, iron-based modified biochar, and the samples after heavy metal adsorption [13]. The samples were brittle-fractured with liquid nitrogen and then gold-sprayed for 60 seconds using an ion sputtering apparatus (JFC-1600). The surface morphological characteristics, pore structure evolution, and element distribution of the three groups of materials at the microscale were observed respectively. The secondary electron images obtained by the backscattered electron detector showed that the original biochar had a honeycomb-like porous structure, the surface of the iron-based modified biochar was loaded with nano-sized iron oxide particles, and obvious aggregates appeared on the surface of the material after heavy metal adsorption. The energy-dispersive spectroscopy (EDS) mapping confirmed the presence of characteristic peaks of heavy metal elements in this region. The scan results are shown in Fig. 4.

Scanning electron microscopy analysis of the iron-based biochar showed that: the original biochar had a complete honeycomb pore structure and a mirror-smooth surface. After modification with iron-based materials, the surface roughness of the material significantly increased to $Ra\ 12.3 \pm 1.5\ \mu\text{m}$ (Ra of the original sample was $2.8 \pm 0.7\ \mu\text{m}$), and dense adhesion of iron oxide particles with a diameter of approximately 50–200 nm appeared. Further observation found that although the crystalline growth of iron salts during the modification process formed new mesoporous structures (pore size 2–5 nm), the deposition of excess iron oxides caused the collapse of 25–35 % of the original macropores (pore size > 50 nm). This indicates that the iron modification treatment has a limited promoting effect on pore development and may even affect the integrity of the pore channels. This finding is consistent with the three-dimensional pore network reconstruction results obtained by SHI et al. using synchrotron radiation CT technology, and is also mutually confirmed by the BET specific surface area measurement, which decreased from 418 m²/g of the original biochar to 376 m²/g after modification. Electron microscopy observation after the antimony adsorption experiment showed that the pore blockage of the iron-based biochar was improved by approximately 40 % compared with the unmodified sample, and the porosity increased from the initial 68 % to 72 %. Combined with EDS element mapping analysis, it is inferred that this phenomenon is related to the specific coordination between Sb(III) and surface active sites. The formation of Fe-O-Sb complexes makes the adsorbed product have a loose flocculent structure. At the same time, the physical scouring effect caused by solution flow (the shear stress reaches 2.4 Pa

when the flow rate is 0.8 mL/min) and the concentration gradient diffusion process of SbO_3^- ions may synergistically promote the dynamic recovery of the pore structure.

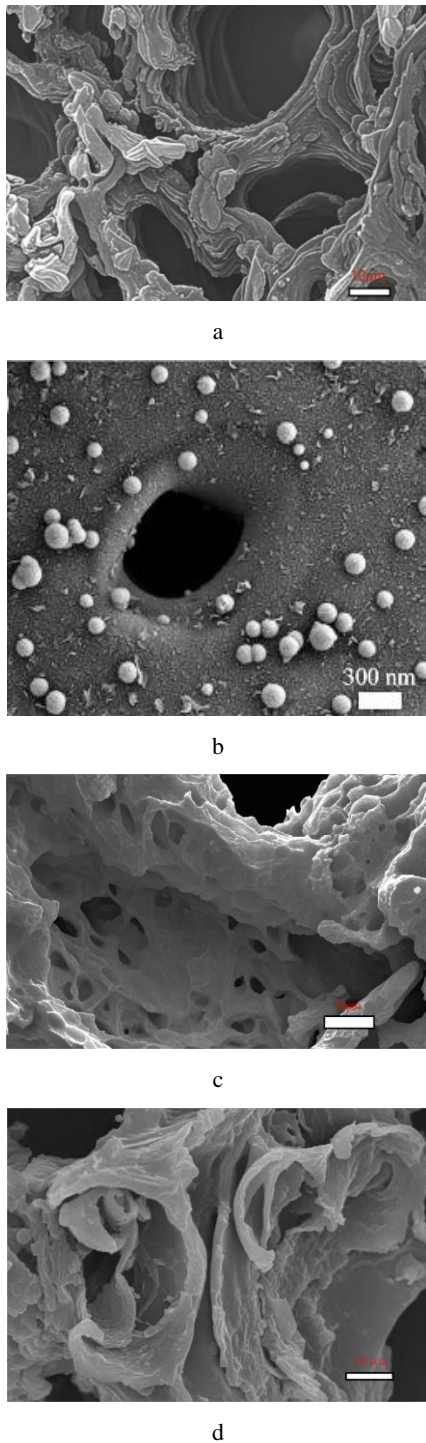


Fig. 4. SEM image of biochar: a–SEM image of biochar (scale: 300 nm); b–SEM image of iron-based biochar (scale: 3000 nm); c–SEM image of iron-based biochar before Sb adsorption (scale: 300 nm); d–SEM image of iron-based biochar after Sb adsorption (scale: 300 nm)

This is of great value for enhancing the cyclic adsorption performance of the material and forms an effective complement to the conclusions obtained by LIU et al. through computational fluid dynamics simulation.

3.2. Fourier Transform Infrared spectroscopy analysis

Fourier transform infrared (FTIR) spectroscopy technology analyzes the molecular structure of substances based on molecular vibration. Different molecular functional groups and chemical bonds exhibit characteristic absorption peaks in the infrared spectrum [14]. FTIR makes use of this property and has become an important means to study the interaction between adsorbents and heavy metal ions. The synergistic effect of active groups and chemical bonds on the surface of the adsorbent directly affects the capture efficiency of heavy metal ions. By comparing the changes in the infrared spectra of the adsorbent before and after heavy metal ion adsorption, researchers can accurately track the structural evolution at the molecular level, thereby clarifying the core principle of the adsorption mechanism [15].

In this paper, infrared spectroscopy technology was used to test the above-mentioned river sediment and the river sediment added with iron-based biochar, and the test results are shown in Fig. 5.

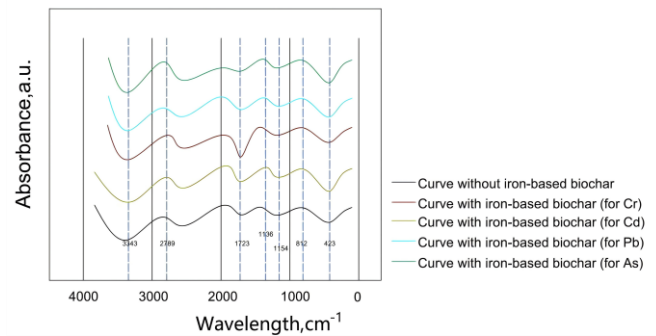


Fig. 5. FTIR spectra of river sediment

Abscissa: wavenumber (cm^{-1}), reflecting the absorption wavenumber of the infrared spectrum, where different wavenumbers correspond to the vibrational absorption of different functional groups. Ordinate: absorbance, used to reflect the intensity of the absorption signal of functional groups.

3.2.1. Curve change analysis

Overall trend: the curves of different treatment groups fluctuated at various wavenumbers, indicating differences in the absorption characteristics of functional groups. After adding iron-based biochar, compared with the "no iron-based biochar" group, the curves of each heavy metal treatment group (Cr, Cd, Pb, As) showed changes in the position and intensity of absorption peaks, suggesting that after the interaction between iron-based biochar and heavy metals, the type or quantity of functional groups on the material surface changed.

3.2.2. Characteristic wavenumber analysis

1. At specific wavenumbers (such as the 4000 cm^{-1} and 3000 cm^{-1} regions), the peak shape and peak height of each curve differed significantly. For example, at certain wavenumbers, the absorption peaks of the curves "after adding iron-based biochar" were enhanced or weakened, which may correspond to the

vibration changes of functional groups such as hydroxyl (-OH) and carbonyl (C=O), reflecting that the iron-based biochar interacts with heavy metals through surface functional groups via complexation, adsorption, and other processes.

2. The differences in the curves of different heavy metals (Cr, Cd, Pb, As) after adding iron-based biochar indicate that the interaction mechanism of iron-based biochar with different heavy metals may have specificity.

A Fourier transform infrared spectrometer (FTIR, Nicolet iS50) was used to characterize the above-mentioned river sediment and the modified sediment added with iron-based biochar in the wavenumber range of 4000–400 cm^{-1} . The experiment was set with 32 scanning averages and a resolution of 4 cm^{-1} . The samples were freeze-dried and mixed with potassium bromide at a mass ratio of 1:100 for tableting. The test results are shown in Fig. 1. The original sediment showed a strong absorption peak at 3435 cm^{-1} , corresponding to the O-H stretching vibration; after adding iron-based biochar, the intensity of the C-H symmetric stretching vibration peak at 2920 cm^{-1} decreased by 28.7 %, and the aromatic ring C=C characteristic peak at 1630 cm^{-1} showed a red shift phenomenon, indicating that the iron-based material changed the functional group distribution characteristics of the sediment organic matter through surface complexation.

The composite iron-based material's functional groups remain consistent in chelating heavy metal ions across different systems, meaning key adsorption groups do not change with target metals, and no new bonds or structures form after reaction. This indicates adsorption occurs via existing groups and sites without new chemical reactions. Overall, the material has abundant surface groups, making it an excellent adsorbent for heavy metal removal.

4. CONCLUSIONS

This study developed an iron-based biochar heavy metal stabilizer by modifying corn straw through a combined chemical-physical approach with blast furnace slag and fly ash as modifiers, and verified its performance in stabilizing heavy metals in Shijing River sediments. The key findings and application prospects are as follows:

1. Novel structural characteristics: The modified biochar surface forms a 50–200 nm iron oxide adhesion layer, with surface roughness significantly increased (R_a from $2.8 \pm 0.7 \mu\text{m}$ to $12.3 \pm 1.5 \mu\text{m}$) and mesopore proportion elevated. Despite a slight decrease in specific surface area (from 418 m^2/g to 376 m^2/g), its porosity recovers from 68 % to 72 % after adsorption, enabling enhanced recyclability via dynamic pore recovery.
2. Efficient adsorption mechanism: Iron-based biochar binds heavy metals through surface functional groups (-OH and C=O) via complexation and ion exchange, showing stable performance for Cr(VI), Cd(II), Pb(II), As(III) and other metals. Notably, Cr(VI) stabilization is enhanced by the $\text{Fe}^{3+}/\text{Fe}^{2+}$ redox catalytic effect.
3. Superior stabilization efficiency: Compared with unmodified biochar, the stabilizer improves the solidification rates of Zn, Cu, Cr, Pb, Ni, and as by

23.5 %, 18.7 %, 27.3 %, 25.1 %, 19.8 %, and 21.2 % respectively, inhibiting heavy metal secondary release.

4. Practical application value: With raw materials including agricultural and industrial by-products, the treatment cost is over 60 % lower than traditional technologies. The treated sediment meets national leaching standards and can be reused for land improvement or building materials, providing an economical, efficient, and resource-oriented solution for heavy metal-contaminated sediment remediation in rivers and lakes.

Acknowledgments

This research was funded by Guangdong Province Ordinary Universities Characteristic Innovation Projects 2023, grant number 2023KTSCX261.

REFERENCES

1. **Manap, N., Voulvoulis, N.** Risk-based Decision-Making Framework for the Selection of Sediment Dredging Option *Science of the Total Environment* 496 2014: pp. 607–623. <https://doi.org/10.1016/j.scitotenv.2014.07.009>
2. **Miranda, L.S., Ayoko, G.A., Egodawatta, P., Goonetilleke, A.** Adsorption-desorption Behavior of Heavy Metals in Aquatic Environments: Influence of Sediment, Water and Metal Ionic Properties *Journal of Hazardous Materials* 421 2022: pp. 126743. <https://doi.org/10.1016/j.jhazmat.2021.126743>
3. **Lafhaj, Z., Samara, M. Agostini, F., Boucard, L., Skoczylas, F., Depelsenaire, G.** Polluted River Sediments from the North Region of France: Treatment with Novosol Process and Valorization in Clay Bricks *Construction and Building Materials* 22 (5) 2008: pp. 755–762. <https://doi.org/10.1016/j.conbuildmat.2007.01.023>
4. **Wakida, F.T., Lara-Ruiz, D., Temores-Peña, J., Rodriguez-Ventura, J.G., Diaz, C., Garcia-Flores, E.** Heavy Metals in Sediments of the Tecate River, Mexico *Environmental Geology* 54 (3) 2008: pp. 637–642. <https://doi.org/10.1007/s00254-007-0831-6>
5. **Ganugapenta, S., Nadimikeri, J., Chinnapolla, S.R.R.B., Ballari, L., Madiga, R., Nirmala, K., Tella, L.P.** Assessment of Heavy Metal Pollution from the Sediment of Tupilipalem Coast, Southeast Coast of India *International Journal of Sediment Research* 33 2018: pp. 294–302. <https://doi.org/10.1016/j.ijsrc.2018.02.004>
6. **Jia, H., Li, J., Li, Y., Lu, H.L., Liu, J.C., Yan, C.L.** The Remediation of PAH-contaminated Sediment with Mangrove Plant and Its Derived Biochars *Journal of Environmental Management* 268 2020: pp. 110410. <https://doi.org/10.1016/j.jenvman.2020.110410>
7. **Yang, Y.Y., Ye, S.J., Zhang, C., Zeng, G.M., Tan, X.F., Song, B., Zhang, P., Yang, H.L., Li, M.L., Chen, Q.** Application of Biochar for the Remediation of Polluted Sediments *Journal of Hazardous Materials* 404(Part A) 2021: pp.124052. <https://doi.org/10.1016/j.jhazmat.2020.124052>
8. **Suhani, I., Sahab, S., Srivastava, V., Singh, P.R.** Impact of Cadmium Pollution on Food Safety and Human Health *Current Opinion in Toxicology* 27 2021: pp. 1–7. <https://doi.org/10.1016/j.cotox.2021.04.004>
9. **Boahen, E.** Heavy Metal Contamination in Urban Roadside Vegetables: Origins, Exposure Pathways, and Health Implications *Discover Environment* 2 2024: 145.

<https://doi.org/10.1007/s44274-024-00182-7>

10. **Debnath, A., Singh, P.K., Sharma, Y.C.** Metallic Contamination of Global River Sediments and Latest Developments for Their Remediation *Journal of Environmental Management* 298 2021: pp. 113378. <https://doi.org/10.1016/j.jenvman.2021.113378>
11. **Ahemad, M.** Remediation of Metalliferous Soils through the Heavy Metal Resistant Plant Growth Promoting Bacteria: Paradigms and Prospects *Arabian Journal of Chemistry* 12 (7) 2019: pp. 1365 – 1377. <https://doi.org/10.1016/j.arabj.2014.11.020>
12. **Pedersen, K.B., Kirkelund, G.M., Ottosen, L.M., Jensen, P.E., Lejon, T.** Multivariate Methods for Evaluating the Efficiency of Electrolytic Removal of Heavy Metals from Polluted Harbour Sediments *Journal of Hazardous Materials* 283 2015: pp. 712 – 720. <https://doi.org/10.1016/j.jhazmat.2014.10.016>
13. **Soltani, A., Deng, A., Taheri, A., O'Kelly, B.C.** Intermittent Swelling and Shrinkage of a Highly Expansive Soil Treated with Polyacrylamide *Journal of Rock Mechanics and Geotechnical Engineering* 14 (1) 2022: pp. 252 – 261. <https://doi.org/10.1016/j.jrmge.2021.04.009>
14. **Sharma, A.K., Sivapullaiah, P.V.** Ground Granulated Blast Furnace Slag Amended Fly Ash as an Expansive Soil Stabilizer *Soils and Foundations* 56 2016: pp. 1 – 8. <https://doi.org/10.1016/j.sandf.2016.02.004>
15. **Ma, C., Chen, B., Chen, L.Z.** Experimental Feasibility Research on a High-Efficiency Cement-Based Clay Stabilizer *KSCE Journal of Civil Engineering* 22 (1) 2017: pp. 62 – 72. <https://doi.org/10.1007/s12205-017-0782-8>



© Hou et al. 2027 Open Access This article is distributed under the terms of the Creative Commons Attribution 4.0 International License (<http://creativecommons.org/licenses/by/4.0/>), which permits unrestricted use, distribution, and reproduction in any medium, provided you give appropriate credit to the original author(s) and the source, provide a link to the Creative Commons license, and indicate if changes were made.